Eur. Phys. J. B (2019) 92: 124
https://doi.org/10.1140/epjb/e2019-100107-7

THE EUROPEAN PHYSICAL JOURNAL B

Regular Article

A solvable model of Landau quantization breakdown

Thierry Champel[1,a] and Serge Florens[2]

[1] Université Grenoble Alpes, CNRS, LPMMC, 25 avenue des Martyrs, 38042 Grenoble, France
[2] Université Grenoble Alpes, CNRS, Institut Néel, 25 avenue des Martyrs, 38042 Grenoble, France

Received 25 February 2019 / Received in final form 15 April 2019
Published online 10 June 2019

Abstract. Physics of two-dimensional (2D) electron gases under perpendicular magnetic field often displays three distinct stages when increasing the field amplitude: a low field regime with classical magnetotransport, followed at intermediate field by a Shubnikov–de Haas phase where the transport coefficients present quantum oscillations, and, ultimately, the emergence at high field of the quantum Hall effect with perfect quantization of the Hall resistance. A rigorous demonstration of this general paradigm is still limited by the difficulty in solving models of quantum Hall bars with macroscopic lateral dimensions and smooth disorder. We propose here the exact solution of a simple model exhibiting similarly two sharp transitions that are triggered by the competition of cyclotron motion and potential-induced drift. As a function of increasing magnetic field, one observes indeed three distinct phases showing respectively fully broken, partially smeared, or perfect Landau level quantization. This model is based on a non-rotationally invariant, inverted 2D harmonic potential, from which a full quantum solution is obtained using 4D phase space quantization. The developed formalism unifies all three possible regimes under a single analytical theory, as well as arbitrary quadratic potentials, for all magnetic field values.

1 Introduction

Magneto-transport in two-dimensional (2D) electronic gases at low temperatures presents ubiquitous features that are observed in vastly different classes of systems, from semiconducting heterostructures [1] to graphene [2–4] and other carbon-based materials, oxide interfaces [5], and topological systems [6]. While details in the transport characteristics will strongly depend on the peculiarities of a given material (for instance the sign of magnetoconductance variation at low field, or the value of Hall conductance quantization plateaus), Landau level formation (or its counterpart at decreasing field, Landau level breakdown) appears as a very generic phenomenon. Indeed, Landau levels start to be witnessed only from an intermediate magnetic field regime, in which mild oscillation of thermodynamic and transport coefficients are observed. Only in a second range [7,8] of even higher magnetic field does full quantization of the Hall conductance finally emerge, with the Landau level index becoming a good quantum number.

In order to explain these observations, the electronic motion in a perpendicular magnetic field and subject to confining or disordered electrostatic potentials has been thoroughly studied by many different theoretical methods [9–19]. One clear limitation of current theories is their inability to comprehend all regimes of magnetic field (from low to intermediate and high) in a unified way, so that the question of the sharpness of the transitions between each regime is not easily established on general grounds.

Our goal in this paper is to propose an exactly solvable model of Landau quantization breakdown that exhibits clearly two sharp transitions. This simple model is based on a non-rotationally invariant and inverted 2D parabolic potential, that we exactly solve in two dimensions for all values of the perpendicular magnetic field. Two mathematically related but physically distinct quadratic potential models are already well-known from the literature. The first model [20,21], often used to describe quantum dots, considers a fully confining 2D parabolic potential, and was solved around the same time as the Landau states [22] for the free motion problem. This solution led to the Fock–Darwin eigenstates [20,21], showing a discrete energy spectrum for all magnetic field values. Indeed, the effect of finite magnetic field amounts to redefine the quantum states while renormalizing the harmonic spectrum. The second model, relevant for quantum point contacts, was proposed and solved decades later by Fertig and Halperin [23], who considered quantum motion in a quadratic saddle point potential. The mathematical solution is here more involved due to the use of scattering states in a potential that is unbounded from below. Again, this model presents the same feature that the physics is weakly dependent on magnetic field, with tunneling being mostly renormalized by cyclotron motion [24]. In contrast, we will find that the inverted non-rotationally invariant quadratic potential, which is relevant to describe antidots

[a] e-mail: thierry.champel@grenoble.cnrs.fr

or Coulomb impurities at a local level, displays markedly different electronic states from the low to intermediate and finally high magnetic field regimes. While this 2D inverted parabolic potential model could be solved by wavefunction techniques (adapted to each specific magnetic field range), or using more general path integral approaches [25–28], we propose here an analytic and unified phase space solution that naturally encompasses all field ranges. As a matter of fact, this single solution also accounts for the Fock–Darwin wavefunctions and Fertig–Halperin scattering states in the case where the sign of two or one curvatures of the potential is inversed, respectively. We note that the case of an inverted one-dimensional (1D) parabolic potential was recently solved using special functions [29], and displays a similar albeit simpler phenomenology compared to the 2D situation with a finite magnetic field.

The approach that we follow here extends previous phase space quantization ideas [30,31] that were used to derive semiclassical approximations in the large magnetic field limit [32–35], allowing good understanding of local density of states measurements [36,37] in the quantum Hall regime. This formalism, best suitable at high field, relies upon wavefunctions that are eigenstates of the free Hamiltonian (with pure Landau level spectrum), while maintaining a semiclassical behavior through their coherent state character with respect to the guiding center coordinate (displaying hence a 2D phase space). This property allows one to easily perform the projection of any states of the Hilbert space onto a given arbitrary Landau level, a procedure which assumes a full energy decoupling between the orbital and guiding center degrees of freedom of the electron in the plane. The semiclassical-type approximations are then vindicated at high magnetic fields by the slow dynamics of the guiding center.

The main technical development made in the present paper is an extension of the coherent state formalism to account efficiently for Landau level mixing. Such a mixing inherently induced by a nonuniform electrostatic potential signals that the Landau level index may not be a good quantum number anymore, and that the cyclotron motion can in general not be treated independently of the guiding center motion. The key physical insight relies on the use of a four-dimensional (4D) phase space, which allows one to treat both orbital motion and guiding center drifting on an equal footing. This approach relies on the general dynamics of phase space distribution functions, which has been proved to be an autonomous formulation of quantum mechanics [38–40]. After establishing the general formalism describing the dynamics for the corresponding 4D Wigner functions, we obtain a unique compact analytical solution for the case of an arbitrary quadratic potential, accounting for the three different physical situations discussed above (quantum dots, quantum point contacts, and quantum antidots). The case of a quantum antidot is found to display rich physics as a function of magnetic field. The strong magnetic field regime where both orbital and guiding center motions are associated with discrete energy levels gets substituted below a critical magnetic field by a regime with broadened Landau and antidot energy levels, before an ultimate breakdown of guiding center and orbital motions at very low magnetic fields. The behavior shown by our toy model of quantum antidot is clearly relevant for the understanding of the quantum Hall effect breakdown occurring in the more complicated case of a random potential.

The plan is organized as follows. For completeness, Section 2 briefly reviews the high magnetic field coherent state formalism and the general equations determining the electronic motion in the corresponding 2D coherent state representation. Since the Landau level index is not a good quantum number at any finite magnetic fields, it becomes relevant in general to replace this discrete quantum number by an extra continuous degree of freedom with coherent state character, in the same way as for the guiding center degree of freedom. This leads us to work preferentially in a full 4D phase space representation provided by a basis of doubly coherent states [41–44]. Section 3 provides the derivation of the general equation describing electronic motion in the plane under a perpendicular magnetic field within a 4D phase space representation (technical details are provided in Appendix A). The full quantum equation is solved in Section 4 for the case of arbitrary quadratic electrostatic potentials in terms of two independent *effective* cyclotron and guiding center motions. Remarkably, in the full 4D phase-space representation, all types of quadratic potential enjoy a generic (unique) and compact exact quantum solution, which is valid at any magnetic fields. The physics of the seldom considered inverted parabolic potential is investigated in Section 5, as a model of Landau quantization breakdown.

2 Review of the 2D-coherent state representation

In this paper, we consider a single electron of charge $e = -|e|$ and effective mass m^* at position $\mathbf{r} = (x, y)$ in a 2D plane subject to a perpendicular uniform magnetic field $\mathbf{B} = B\hat{\mathbf{z}}$ and an electrostatic potential $V(\mathbf{r})$. The Hamiltonian reads

$$H = \frac{1}{2m^*}\left(-i\hbar\boldsymbol{\nabla}_{\mathbf{r}} - e\mathbf{A}(\mathbf{r})\right)^2 + V(\mathbf{r}), \tag{1}$$

where the vector potential $\mathbf{A}(\mathbf{r})$ is related to the magnetic field with the equation $\boldsymbol{\nabla} \times \mathbf{A} = \mathbf{B}$. In the absence of potential [i.e., for $V(\mathbf{r}) = 0$], the corresponding quantum mechanical problem can be readily solved and yields the well-known quantization of the kinetic energy into discrete Landau levels $E_n = (n + 1/2)\hbar\omega_c$ where n is a positive integer (a.k.a. the Landau level index) and ω_c is the cyclotron frequency proportional to the magnetic field amplitude B as $\omega_c = |e|B/m^*$. Owing to the degeneracy of the kinetic energy levels, it is possible to showcase different bases of eigenstates associated with this Landau level quantization.

A physically transparent basis is provided by the vortex set of states [30,31] expressed in the symmetrical gauge $\mathbf{A} = \mathbf{B} \times \mathbf{r}/2$ as

$$\langle \mathbf{r}|n, \mathbf{R}\rangle = \frac{1}{l_B\sqrt{2\pi n!}}\left(\frac{z - Z}{\sqrt{2}l_B}\right)^n e^{-\frac{|z|^2+|Z|^2-2Zz^*}{4l_B^2}}, \tag{2}$$

where $l_B = \sqrt{\hbar/|e|B}$ is the magnetic length and $z = x + iy$ refers to the electron position in the complex plane. Within this peculiar set of eigenstates of the Landau level problem, the degeneracy quantum number is provided by the vortex position $\mathbf{R} = (X, Y)$, associated with the complex coordinate $Z = X + iY$ in the complex plane, which uniquely characterizes for $n \geq 1$ the location of the zeros of the wave function in the 2D plane. In the limit of vanishing l_B the positions $\mathbf{R}$ reduce to the classical guiding center location. Despite presenting a nonorthogonal overlap with respect to the quantum number $\mathbf{R}$ typical of coherent states

$$\langle n_1, \mathbf{R}_1 | n_2, \mathbf{R}_2 \rangle = \delta_{n_1,n_2}\, e^{-\frac{|Z_1|^2+|Z_2|^2-2Z_1^* Z_2}{4l_B^2}}, \qquad (3)$$

the states (2) form a coherent state basis with respect to the guiding center coordinate (within each Landau level), obeying the completeness relation

$$\int \frac{d^2\mathbf{R}}{2\pi l_B^2} \sum_{n=0}^{+\infty} |n, \mathbf{R}\rangle\langle n, \mathbf{R}| = 1. \qquad (4)$$

By associating the incremental area $d^2\mathbf{R}$ with the area $2\pi l_B^2$, this relation explicitly points out the degeneracy of the Landau levels to be $(2\pi l_B^2)^{-1}$ per unit area.

This Landau level degeneracy gets lifted when considering a non-uniform potential $V(\mathbf{r})$. At high magnetic fields, i.e., when Landau level mixing can reasonably be neglected, the degeneracy lifting process becomes nonperturbative in nature and is the source of theoretical difficulties. The continuous character of the degeneracy quantum number $\mathbf{R}$ in the vortex state basis $|n, \mathbf{R}\rangle$ then offers a differential perspective of this process by an arbitrary potential, which has been thoroughly studied during the last decade in a series of papers [32,34,35]. Due to the coherent state nature of the degree of freedom $\mathbf{R}$, the electronic Green's function in the time domain t corresponding to Hamiltonian (1) can be written as the convolution

$$G(\mathbf{r}, \mathbf{r}'; t) = \int \frac{d^2\mathbf{R}}{2\pi l_B^2} \sum_{n_1,n_2} K_{n_1,n_2}(\mathbf{r}, \mathbf{r}'; \mathbf{R})\, g_{n_1,n_2}(\mathbf{R}; t) \qquad (5)$$

where the electronic structure factor defined by

$$K_{n_1,n_2}(\mathbf{r}, \mathbf{r}'; \mathbf{R}) = e^{-(l_B^2/4)\Delta_{\mathbf{R}}} \left[\langle n_2, \mathbf{R}|\mathbf{r}'\rangle \langle \mathbf{r}|n_1, \mathbf{R}\rangle\right] \qquad (6)$$

is independent of the electrostatic potential $V(\mathbf{r})$ and embodies the quantum contribution arising from the pure orbital motion of the electron (here $\Delta_{\mathbf{R}}$ is the Laplacian operator taken with respect to the position $\mathbf{R}$). The vortex Green's function components $g_{n_1,n_2}(\mathbf{R}; t)$, which encode the quantum drift of the guiding center induced by $V(\mathbf{r})$, obey the equations

$$\left(i\hbar\partial_t - E_{n_1} \pm i0^+\right) g_{n_1,n_2}(\mathbf{R}; t) - \sum_{n_3} v_{n_1,n_3}(\mathbf{R}) \star_{\mathbf{R}} g_{n_3,n_2}(\mathbf{R}; t) = \delta_{n_1,n_2}\delta(t) \qquad (7)$$

with the effective potential matrix elements

$$v_{n_1,n_2}(\mathbf{R}) = \int d^2\mathbf{r}\, K_{n_1,n_2}(\mathbf{r}, \mathbf{r}; \mathbf{R})\, V(\mathbf{r}) \qquad (8)$$

expressing the average of the bare potential $V(\mathbf{r})$ over the quantized orbital motion. Here, the infinitesimal quantity $\pm 0^+$ relates to the retarded or advanced Green's functions. The symbol $\star_{\mathbf{R}}$ is a pseudodifferential infinite-order symplectic operator

$$\star_{\mathbf{R}} = \exp\left[i\frac{l_B^2}{2}\left(\overleftarrow{\partial}_X \overrightarrow{\partial}_Y - \overleftarrow{\partial}_Y \overrightarrow{\partial}_X\right)\right], \qquad (9)$$

where the arrows above the partial derivatives indicate to which side (left or right) they have to be applied. It is a magnetic version of the Groenewold–Moyal star product [40], with l_B^2 playing the role of an effective Planck's constant and the 1D conjugated variables, position and momentum, being replaced by the components X and Y of the orbit center in the 2D plane.

The exact expression (5) translates into the quantum mechanical language the natural decomposition of the electronic motion into orbital and orbit center degrees of freedom. The vortex representation introducing both discrete and continuous quantum numbers turns out to be well-suited to treat quantitatively the resulting electronic dynamics at high magnetic fields, since it structurally encodes that these two elementary motions are characterized by very different time scales: the fast orbital degree of freedom is described in discrete terms, while a continuous classical phase space representation of the Landau level degeneracy is vindicated by the slow dynamics of the orbit center. In the high magnetic field regime, a good (perturbative) approximation is to entirely separate these two time scales by considering that the orbital motion gets decoupled from the guiding center motion. Technically, this implies restricting the electron dynamics to a given Landau level subspace. This state projection is conveniently performed for any Landau levels through the analyticity property of the vortex state basis (2) in the complex guiding center variable Z, which holds irrespective of the Landau level index n (in contrast, the well-known anti-analyticity property of the wave functions in the electronic variable z only holds for the lowest Landau level). In terms of vortex Green's functions, only diagonal elements $g_{n_1,n_1}(\mathbf{R}; t)$ contribute to the overall electron dynamics in expression (5) after projection. Then, at the level of the guiding center motion, the star product operator (9) generates a hierarchy of local energy scales ordered by powers of l_B^2 and successive spatial derivatives of the effective potential (8), which allows one to devise semiclassical nonperturbative approximation schemes for the vortex Green's functions $g_{n_1,n_1}(\mathbf{R}; t)$ valid at small times t (and physically justified at finite temperatures).

The objective of this paper is to address the situation beyond the Landau level projection, i.e., to eventually relax the high magnetic field constraint. This means to deal in equation (7) with the entire matrix structure of the vortex Green's functions associated to the Landau levels

together with the differential aspects related to the guiding center dependence. In the following, we shall develop an alternative strategy valid at any magnetic fields, which requires a reformulation of the quantum representation of the states.

3 General equation of motion in the 4D-coherent state representation

The idea is to treat the two electronic degrees of freedom associated to the cyclotron motion and the guiding center motion on an equal footing, i.e., within a fully differential 4D phase-space perspective. For this purpose, we introduce a coherent state representation of the orbital degree of freedom by defining the doubly coherent states $|\boldsymbol{\rho},\mathbf{R}\rangle$, built from the vortex states as

$$|\boldsymbol{\rho},\mathbf{R}\rangle = e^{-\frac{|\zeta|^2}{4l_B^2}} \sum_{n=0}^{+\infty} \frac{1}{\sqrt{n!}} \left(\frac{\zeta^*}{\sqrt{2}l_B}\right)^n |n,\mathbf{R}\rangle, \tag{10}$$

where the orbital position $\boldsymbol{\rho}=(\rho_x,\rho_y)$ replaces the quantized Landau level index n by a continuous cyclotron motion around the guiding center $\boldsymbol{R}$ in the 2D plane, with $\zeta=\rho_x+i\rho_y$ its complex number representation (thus $\zeta^*=\rho_x-i\rho_y$). It can be easily established that this set of states form a bi-coherent states basis, with the standard non-orthogonal overlap expression:

$$\begin{aligned}\langle\boldsymbol{\rho}_1,\mathbf{R}_1|\boldsymbol{\rho}_2,\mathbf{R}_2\rangle &= \langle\boldsymbol{\rho}_1|\boldsymbol{\rho}_2\rangle\,\langle\mathbf{R}_1|\mathbf{R}_2\rangle \\ &= e^{-\frac{|\zeta_1|^2+|\zeta_2|^2-2\zeta_1\zeta_2^*}{4l_B^2}} e^{-\frac{|Z_1|^2+|Z_2|^2-2Z_1^*Z_2}{4l_B^2}},\end{aligned} \tag{11}$$

and the completeness relation

$$\int\frac{d^2\mathbf{R}}{2\pi l_B^2}\int\frac{d^2\boldsymbol{\rho}}{2\pi l_B^2}|\boldsymbol{\rho},\mathbf{R}\rangle\langle\boldsymbol{\rho},\mathbf{R}| = 1. \tag{12}$$

From equations (2) and (10) one easily gets the expression for the fully coherent wave function (which already appeared in the literature several decades ago, see e.g. Refs. [41,42])

$$\langle\mathbf{r}|\boldsymbol{\rho},\mathbf{R}\rangle = \frac{1}{l_B\sqrt{2\pi}} e^{-\frac{|z|^2+|Z|^2+|\zeta|^2-2Z(z^*-\zeta^*)-2z\zeta^*}{4l_B^2}}. \tag{13}$$

The corresponding Green's functions in this representation of bi-coherent states are obtained from the vortex Green's functions components via a simple change of basis as

$$\begin{aligned}g_{\boldsymbol{\rho}_1,\boldsymbol{\rho}_2}(\mathbf{R};t) = e^{-\frac{|\zeta_1|^2+|\zeta_2|^2}{4l_B^2}} \sum_{n_1=0}^{+\infty}\sum_{n_2=0}^{+\infty} \left(\frac{\zeta_1}{\sqrt{2}l_B}\right)^{n_1} \\ \times \left(\frac{\zeta_2^*}{\sqrt{2}l_B}\right)^{n_2} \frac{g_{n_1,n_2}(\mathbf{R};t)}{\sqrt{n_1!\,n_2!}}.\end{aligned} \tag{14}$$

The analytical dependence of these functions on the variables ζ_1 and ζ_2^* is put to good use in order to write down a general "diagonal" expression for the electronic Green's function (see Appendix A for a detailed derivation) similarly to equation (5)

$$G(\mathbf{r},\mathbf{r}';t) = \int\frac{d^2\mathbf{R}}{2\pi l_B^2}\int\frac{d^2\boldsymbol{\rho}}{2\pi l_B^2} K(\mathbf{r},\mathbf{r}';\boldsymbol{\rho},\mathbf{R})\, g(\boldsymbol{\rho},\mathbf{R};t) \tag{15}$$

with the Kernel function

$$K(\mathbf{r},\mathbf{r}';\boldsymbol{\rho},\mathbf{R}) = e^{-(l_B^2/4)(\Delta_{\mathbf{R}}+\Delta_{\boldsymbol{\rho}})}\,[\langle\boldsymbol{\rho},\mathbf{R}|\mathbf{r}'\rangle\,\langle\mathbf{r}|\boldsymbol{\rho},\mathbf{R}\rangle], \tag{16}$$

and where the diagonal component functions $g(\boldsymbol{\rho},\mathbf{R};t)$ obey the relatively compact (exact) equation

$$\left(i\hbar\partial_t \pm i0^+\right) g(\boldsymbol{\rho},\mathbf{R};t) - E(\boldsymbol{\rho},\mathbf{R}) \star_{\mathbf{R}} \star_{\boldsymbol{\rho}} g(\boldsymbol{\rho},\mathbf{R};t) = \delta(t). \tag{17}$$

The matrix structure encountered into the previous system of equation (7) has been replaced in the present 4D phase space representation by the presence of an additional pseudodifferential infinite-order symplectic operator

$$\star_{\boldsymbol{\rho}} = \exp\left[i\frac{l_B^2}{2}\left(\overleftarrow{\partial}_{\rho_x}\overrightarrow{\partial}_{\rho_y} - \overleftarrow{\partial}_{\rho_y}\overrightarrow{\partial}_{\rho_x}\right)\right], \tag{18}$$

whose structure is the same as that of the star product operator $\star_{\mathbf{R}}$ which governs the quantum motion of the guiding center $\mathbf{R}$. Here, the quantity $E(\boldsymbol{\rho},\mathbf{R})$ expresses the classical total energy

$$E(\boldsymbol{\rho},\mathbf{R}) = \frac{1}{2}m^*\omega_c^2\boldsymbol{\rho}^2 + V(\boldsymbol{\rho}+\mathbf{R}), \tag{19}$$

which includes both the classical (rotational) kinetic energy contribution (which was previously associated with the Landau levels) and the potential energy contribution. Expression (19) is obvious on semiclassical grounds, and the only difficulty brought by quantum mechanics in its 4D phase space representation is the necessity to deal with the star-product (18).

The full phase space formulation provided by the use of the bi-coherent state set thus offers a physically transparent perspective, with the explicit implementation of the electron motion decomposition $\mathbf{r}=\boldsymbol{\rho}+\mathbf{R}$ in the quantum realm. Note that the 4D phase space is characterized here by two spatial coordinates $\boldsymbol{\rho}$ and $\boldsymbol{R}$, in contrast to the more standard phase space representation with electronic coordinate $\boldsymbol{r}$ and its zero-field conjugate momentum $\boldsymbol{p}=-i\hbar\nabla$. In fact, under a finite magnetic field, the canonical quantization readily shows that (X,Y) and (ρ_x,ρ_y) each constitute a quantum conjugate pair, vindicating our choice of 4D phase space representation. As a consequence, the main difficulty in this deformation quantization formulation is entirely embodied in the infinite-order differential operators $\star_{\mathbf{R}}$ and $\star_{\boldsymbol{\rho}}$ appearing in equation (17). In general, the electronic potential energy term $V(\mathbf{r})$ introduces a coupling between the orbital $\boldsymbol{\rho}$ and the guiding center $\mathbf{R}$ degrees of freedom, which makes this quantum problem generically quite complicated to solve. Nevertheless, as shown in the next section, an exact decoupling can be handled for any quadratic potentials.

4 Generic solution for arbitrary quadratic potentials

So far, we have derived the general quantum equation (17) obeyed by the Green's functions in the 4D phase space representation, without resorting to any specific form for the potential $V(\mathbf{r})$. The case of a linear potential term does not present peculiar difficulties, since it does not lead to a coupling between the orbital and guiding center degrees of freedom. Consequently, from now on we focus on the case of quadratic potentials which can be written without loss of generality (a translation and a rotation of the coordinates lead immediately to the most generic quadratic form) as

$$V(\mathbf{r}) = ax^2 + by^2, \tag{20}$$

where a and b are arbitrary real coefficients, which encompass the three possible cases of potentials: (i) confining (parabolic case, $a > 0$ and $b > 0$); (ii) saddle point (hyperbolic case, $ab < 0$); and (iii) impurity-like (inverted parabolic case, $a < 0$ and $b < 0$). Therefore, the total energy (19) reads

$$E(\boldsymbol{\rho}, \mathbf{R}) = a(X + \rho_x)^2 + b(Y + \rho_y)^2 + c\boldsymbol{\rho}^2 \tag{21}$$

with $c = \frac{1}{2}m^*\omega_c^2$. The difficulty obviously comes from the presence of terms mixing the $\boldsymbol{\rho}$ and $\mathbf{R}$ coordinates, a hallmark of quadratic (squared) contributions.

The above equation (17) for the phase space Green's functions can be solved exactly through the introduction of a well-chosen change in variables $(\boldsymbol{\rho}, \mathbf{R}) \to (\mathbf{R}_1, \mathbf{R}_2)$, which allows us to simultaneously decouple the spatial dependences in the total energy and in the differential star-operators. More explicitly, we impose that the total energy reads after the variable transformation as

$$E(\boldsymbol{\rho}, \mathbf{R}) = V_1(\mathbf{R}_1) + V_2(\mathbf{R}_2), \tag{22}$$

where the new (quadratic) potential functions V_1 and V_2 will be determined later on. A second condition is that the new star-products $\star_{\mathbf{R}_1}$ and $\star_{\mathbf{R}_2}$ defined with respect to the new variables $\mathbf{R}_1$ and $\mathbf{R}_2$ remain decoupled (typically, we do not want to generate cross-derivative terms like $\overleftarrow{\partial}_{X_1}\overrightarrow{\partial}_{Y_2}$). The solutions to the differential equations in $\mathbf{R}_1$ and $\mathbf{R}_2$ are then derived separately (without the $\delta(t)$ source term) and are appointed in the following as the functions $f_1(\mathbf{R}_1; t)$ and $f_2(\mathbf{R}_2; t)$ with the property that $f_1(\mathbf{R}_1; 0) = f_2(\mathbf{R}_2; 0) = 1$. Hence, it can be easily shown that the full solution of equation (17) is given by the product function

$$g(\boldsymbol{\rho}, \mathbf{R}; t) = \mp i\theta(\pm t)\, f_1(\mathbf{R}_1; t) f_2(\mathbf{R}_2; t) \tag{23}$$

with $\theta(t)$ the Heaviside step function, and where the functions $f_j(\mathbf{R}_j; t)$ with $j = 1$ or 2 obey the equation

$$\left(i\hbar\partial_t \pm i0^+\right) f_j(\mathbf{R}_j; t) - V_j(\mathbf{R}_j) \star_{\mathbf{R}_j} f_j(\mathbf{R}_j; t) = 0. \tag{24}$$

This latter equation is very similar to the one obtained for the pure (decoupled) guiding center motion at high magnetic fields after Landau level projection. We can thus follow the derivation detailed in reference [34] to directly write down the solution

$$f_j(\mathbf{R}_j; t) = \frac{e^{-i[V_j(\mathbf{R}_j) - V_j(\mathbf{R}_{j0})]\tau_j(t)}}{\cos\left[\sqrt{\gamma_j}t/\hbar\right]}\, e^{-\frac{it}{\hbar}\left[V_j(\mathbf{R}_{j0}) \mp i0^+\right]}, \tag{25}$$

where

$$\tau_j(t) = \frac{1}{\sqrt{\gamma_j}} \tan\left(\sqrt{\gamma_j}t/\hbar\right). \tag{26}$$

Here, the point $\mathbf{R}_{j0}$ refers to the critical point of the quadratic potential V_j, i.e., $\boldsymbol{\nabla}_{\mathbf{R}_j} V_j(\mathbf{R}_j)\big|_{\mathbf{R}_j = \mathbf{R}_{j0}} = \mathbf{0}$, and the (uniform) quantity γ_j is related to the Gaussian curvature of the potential V_j as

$$\gamma_j = \frac{l_B^4}{4}\left[\partial_{X_j}^2 V_j \partial_{Y_j}^2 V_j - \left(\partial_{X_j}\partial_{Y_j} V_j\right)^2\right]. \tag{27}$$

This quantity plays a pivotal role, since its square root crucially determines the relative time dependence of the Green's function, and thus the spectral properties of the electronic motion. For instance, when γ_j is real positive, the function $f_j(\mathbf{R}_j; t)$ contains a periodical dependence in time, which can be restated as a Fourier series expansion to yield the alternative expression

$$f_j(\mathbf{R}_j; t) = \sum_{p_j = -\infty}^{+\infty} a_{p_j}(\mathbf{R}_j)\, e^{\frac{it}{\hbar}\left[p_j\sqrt{\gamma_j} - V_j(\mathbf{R}_{j0}) \pm i0^+\right]}. \tag{28}$$

It has been shown in Appendix A of reference [35] that the series coefficients read

$$a_{p_j}(\mathbf{R}_j) = 2(-1)^{n_j} e^{-|\rho_j(\mathbf{R}_j)|} L_n\left(2|\rho_j(\mathbf{R}_j)|\right), \tag{29}$$

$$\rho_j(\mathbf{R}_j) = \frac{V_j(\mathbf{R}_j) - V_j(\mathbf{R}_{j0})}{\sqrt{\gamma_j}}, \tag{30}$$

whenever $p_j = \chi_j(2n_j + 1)$ with n_j a positive integer and $\chi_j = \pm 1$ whether the potential V_j is convex or concave (here $L_n(x)$ is the Laguerre polynomial of degree n), and $a_{p_j}(\mathbf{R}_j) = 0$ whenever $p_j \neq \chi_j(2n_j + 1)$. From expression (28) valid when $\gamma_j \geq 0$ it is thus readily understood that the energy contribution arising from the potential V_j is quantized with energy gaps given by $2\sqrt{\gamma_j}$. For $\gamma_j < 0$, it is understood in equations (25) and (26) that $\sqrt{\gamma_j} = i\sqrt{-\gamma_j}$, so that the cosine and tangent trigonometric functions transform into their hyperbolic counterparts. As a result, the time periodicity of the Green's function is replaced by a decay on the time scale $1/\sqrt{-\gamma_j}$ due to the cutoff function $1/\cosh(\sqrt{-\gamma_j}t)$, which can be seen as a manifestation of quantum tunneling effects.

From the above requirements on the variables decoupling, it is clear that a linear transformation of the coordinates will fit our purpose. Let us write the original variables in terms of the new ones as

$$\begin{aligned} X &= \lambda(X_1 + \alpha X_2), \qquad & \rho_x &= \lambda(X_2 + \beta X_1), \\ Y &= \lambda(Y_1 + \eta Y_2), \qquad & \rho_y &= \lambda(Y_2 + \delta Y_1), \end{aligned} \tag{31}$$

with $\lambda > 0$. The condition for the absence of cross-terms in the star products yields $\beta = \eta$ and $\alpha = \delta$. Furthermore, we

get $\overleftarrow{\partial}_X \overrightarrow{\partial}_Y - \overleftarrow{\partial}_{\rho_x} \overrightarrow{\partial}_{\rho_y} = \overleftarrow{\partial}_{X_1} \overrightarrow{\partial}_{Y_1} - \overleftarrow{\partial}_{X_2} \overrightarrow{\partial}_{Y_2}$ provided that $\lambda^{-2} = 1 - \alpha\beta$. The other constraint (22) leads to $\beta = \alpha a/b$ with

$$\alpha = -\frac{1}{2a}\left[a+b+c-\sqrt{(a+b+c)^2-4ab}\right]. \quad (32)$$

Note that only this combination is compatible with the equality $a\alpha = b\beta$ (this comes out by considering, e.g., the limit $b \to 0$ which necessarily implies $\alpha \to 0$). From this, we obtain

$$\lambda^2 = \frac{1}{2}\frac{a+b+c+\sqrt{(a+b+c)^2-4ab}}{\sqrt{(a+b+c)^2-4ab}}. \quad (33)$$

The effective quadratic potentials read $V_j(\mathbf{R}_j) = a_j X_j^2 + b_j Y_j^2$ with

$$\begin{aligned} a_1 &= \lambda^2\left[a(1+\beta)^2 + c\beta^2\right] \\ &= \frac{a}{2b}\left[b-a-c+\sqrt{(a+b+c)^2-4ab}\right], \quad (34) \\ b_1 &= \lambda^2\left[b(1+\alpha)^2 + c\alpha^2\right] \\ &= \frac{b}{2a}\left[a-b-c+\sqrt{(a+b+c)^2-4ab}\right], \quad (35) \\ a_2 &= \lambda^2\left[a(1+\alpha)^2 + c\right] \\ &= \frac{1}{2}\left[c+a-b+\sqrt{(a+b+c)^2-4ab}\right], \quad (36) \\ b_2 &= \lambda^2\left[b(1+\beta)^2 + c\right] \\ &= \frac{1}{2}\left[c+b-a+\sqrt{(a+b+c)^2-4ab}\right]. \quad (37) \end{aligned}$$

The new variables are expressed in terms of the original guiding center and orbital coordinates as

$$\begin{aligned} X_1 &= \lambda(X-\alpha\rho_x), \qquad X_2 = \lambda(\rho_x - \beta X), \quad (38) \\ Y_1 &= \lambda(Y-\beta\rho_y), \qquad Y_2 = \lambda(\rho_y - \alpha Y). \quad (39) \end{aligned}$$

By considering the high magnetic field limit $c \gg |a|, |b|$ for which $\lambda = 1$ and $\alpha = \beta = 0$, it is clear that, in general, the degree of freedom $\mathbf{R}_1$ plays the role of an effective guiding center, while $\mathbf{R}_2$ corresponds to an effective orbital degree of freedom. The final explicit solution for arbitrary quadratic potentials can be read off from expression (23) for the 4D phase-space Green's function $g(\boldsymbol{\rho}, \mathbf{R}; t)$, expressed from the functions $f_j(\mathbf{R_j}; t)$ in equation (25), with the coordinates $\mathbf{R_j}$ given in equations (38)–(39) and the effective potentials $V_j(\mathbf{R_j}) = a_j X_j^2 + b_j Y_j^2$ determined by the four coefficients in equations (34)–(37). One remarkable aspect of this general solution is that it does not require the computation of any special functions.

5 Model of Landau quantization breakdown

Let us finally analyze some physical features of the exact quantum solution (23). As underlined above, the Gaussian curvatures γ_1 and γ_2 of the effective potentials V_1 and V_2 are key quantities determining the nature itself of the energy spectrum:

$$\gamma_1 = l_B^4 a_1 b_1 = l_B^4 \frac{c}{2}\left[a+b+c-\sqrt{(a+b+c)^2-4ab}\right], \quad (40)$$

$$\gamma_2 = l_B^4 a_2 b_2 = l_B^4 \frac{c}{2}\left[a+b+c+\sqrt{(a+b+c)^2-4ab}\right]. \quad (41)$$

Note that here $l_B^2 c = \frac{1}{2}\hbar\omega_c \geq 0$, while the coefficients a and b can be chosen positive or negative real numbers depending on the spatial configuration for the original potential energy $V(\mathbf{r})$.

A rich variety of regimes, showing structural changes in the energy spectrum, only takes place when both a and b are negative, corresponding to a toy-model of quantum antidot. Indeed, in the other circumstances (i.e., for $ab < 0$, or for a and b both positive), one always gets a real positive γ_2, which signals the discrete quantization of the effective orbital motion with gaps given by the energy scale $\hbar\Omega_c = 2\sqrt{\gamma_2}$. Landau quantization is thus robust at arbitrary small magnetic field for confining or saddle-point potentials. The renormalization of the cyclotron frequency from ω_c to Ω_c due to the Landau level mixing processes can be translated into a renormalization of the magnetic length l_B by introducing the new length $L = l_B\left(l_B^4 c^2/\gamma_2\right)^{1/4} \equiv l_B\left(\omega_c/\Omega_c\right)^{1/2}$. Moreover, it is instructive to rewrite the curvature of the effective potential V_1 as $\gamma_1 = l_B^4 ab l_B^4 c^2/\gamma_2 \equiv \gamma\left(\omega_c/\Omega_c\right)^2$, with $\gamma = l_B^4 ab$ the Gaussian curvature of the electronic potential energy $V(\mathbf{r})$. This proportionality relation shows that when $\gamma_2 > 0$ the sign of γ_1 dictating the effective guiding center motion is in fact entirely determined by the bare potential curvature. Nevertheless, the effective guiding center follows equipotential lines of the effective potential $V_1(\mathbf{R}_1)$, which, in the presence of Landau level mixing, differ from those of $V(\mathbf{R}_1)$ and evolve in magnetic field.

Focusing now the analysis on the inverted parabolic case (a and b negative), it is clear that both effective potential curvatures γ_1 and γ_2 are real and positive for strong enough magnetic field, as seen by taking the limit of large c in equations (40) and (41). Having $\gamma_2 > 0$ signals robust high magnetic field Landau quantization, while $\gamma_1 > 0$ demonstrates that the effective antidot potential V_1 confines the electronic motion due to the strong Lorentz force, despite the bare antidot potential $V(\mathbf{r})$ of equation (20) being repulsive and unbounded from below. Decreasing the magnetic field, i.e. reducing the value of c, one encounters a first critical value $c_+ = \left(\sqrt{|a|} + \sqrt{|b|}\right)^2$ below which the term under the square root in equations (40) and (41) becomes negative. In this case, both orbital and guiding center effective motions lock into decaying orbits (in a semiclassical viewpoint), leading to a finite broadening of both the Landau and antidot energy levels associated to the finite imaginary parts of the quantities $\sqrt{\gamma_1}$ and $\sqrt{\gamma_2}$. Landau quantization only survives on short time-scales in this field regime, where cyclotron orbits shrink ($\mathrm{Im}[\sqrt{\gamma_2}] > 0$), while the guiding center makes larger and larger loops around the antidot

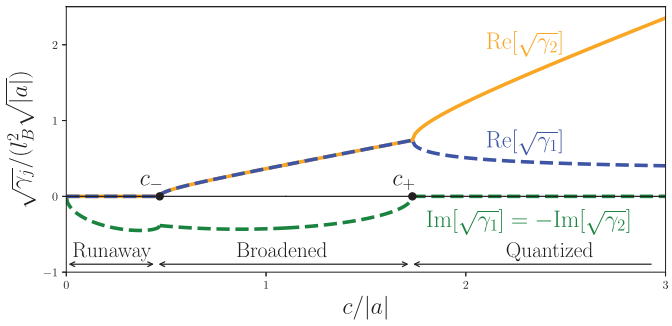

Fig. 1. Dynamical regimes for a nonrotationally invariant antidot. The figure displays the real and imaginary parts of the quantities $\sqrt{\gamma_1}$ and $\sqrt{\gamma_2}$ characterizing the energy spectrum and related to the two effective potentials V_1 and V_2 (defined in Eqs. (34)–(37)), which are associated, respectively, to the effective guiding center coordinate $\boldsymbol{R}_1$ and to the effective orbital motion $\boldsymbol{R}_2$, as a function of the classical cyclotron energy $c = m^*\omega_c^2/2$. Here, an asymmetric inverted parabolic potential with $a = 10\,b < 0$ in equation (20) has been considered. Landau quantization at large magnetic field ($c \geq c_+$) corresponds to real and positive potential curvatures, while the intermediate magnetic field range ($c_- \leq c \leq c_+$) shows broadened Landau and antidot levels due to the non-zero imaginary parts of $\sqrt{\gamma_1}$ and $\sqrt{\gamma_2}$. However, the relation $\mathrm{Im}[\sqrt{\gamma_1}] = -\mathrm{Im}[\sqrt{\gamma_2}]$ translates the fact that the effective cyclotron orbits shrink while the effective guiding center follows orbits that increase as the electron spins down the potential landscape. Finally, both curvatures γ_1 and γ_2 become negative at low magnetic fields ($c \leq c_-$) so that $\sqrt{\gamma_1}$ and $\sqrt{\gamma_2}$ are purely imaginary, corresponding to the electron running down the inverted parabolic potential without performing any cyclotron motion.

potential ($\mathrm{Im}[\sqrt{\gamma_1}] = -\mathrm{Im}[\sqrt{\gamma_2}] < 0$). Finally, when $a \neq b$ so that angular momentum is no more conserved, one finds for lower magnetic fields a second critical value $c_- = (\sqrt{|a|} - \sqrt{|b|})^2$ below which both curvatures γ_1 and γ_2 become real and negative, and thus the quantities $\sqrt{\gamma_1}$ and $\sqrt{\gamma_2}$ get purely imaginary. This low field regime for asymmetric antidot potentials corresponds to the rapid runaway of the electron down the inverted potential without any looping motion from the Lorentz force, so that the magnetic orbital effects are totally washed out. This rich scenario of Landau quantization breakdown in an inverted quadratic potential is illustrated in Figure 1 in the case $a = 10\,b < 0$. Note that the Gaussian curvatures in equations (40) and (41) are purely classical concepts, as the same quantities naturally appear when solving the characteristic Newtonian equation of motion of a charged particle in an arbitrary quadratic potential in presence of a magnetic field. In this sense, the Landau levels breakdown is not intrinsically quantum in nature, although it will affect electronic motion at the quantum level.

6 Conclusion and final remarks

We have developed a 4D phase space representation of the in-plane electronic quantum motion in a perpendicular magnetic field, which is relevant beyond the Landau level projection. While a 2D-coherent state representation considering the discrete Landau level index as a good quantum number still appears efficient at moderately small Landau level mixing, the recourse to a bi-coherent state representation for which both the guiding center and the orbital degrees of freedom are associated with continuous (coherent) quantum numbers turns out to be unavoidable to get phase space solutions describing the electronic quantum motion at any magnetic fields.

As an illustration, we have considered the motion in arbitrary quadratic electrostatic potentials, which is known to be exactly solvable by diagonalization of the Schrödinger's equation. The full phase space formulation (unusual in condensed matter when dealing with fully quantum problems) offers an original viewpoint, with a limpid underlying classical physics, on the quantization processes, which is very different from that provided by the conventional (historical) derivations [20,21,23] based on the wave function formalism. Especially, thanks to the overcompleteness of the coherent state representation, it yields a generic (unique) solution capable to embrace all types of quadratic potential within a simple compact mathematical expression, without having recourse to the properties of special orthogonal (Hermite, Laguerre, etc.) polynomials or special functions as usually required via the wave function formalism. We have also investigated a simplified model of Landau breakdown in the case of an inverted parabolic potential, showing a surprisingly rich phenomenology. Most markedly, this model displays three distinct physical stages when varying the field amplitude, in a very similar way to the situation encountered in disordered 2D electronic gases.

A possible application of the full phase space formalism beyond the case of quadratic potentials may be the derivation of approximate functionals for the local density of states valid in a broader magnetic field range than originally devised in references [34,35] for a smooth disordered electrostatic potential. In particular, one may expect to get specific signatures of Landau level mixing in the characteristic features of the effective guiding center motion. The extension of the phase space formalism may also be useful for the study of the correlations of the local density of states in a broader regime than in reference [45] which neglects Landau level mixing. However, the present phase space formulation, which naturally allows one to perform semiclassical (local) approximations, is usually not convenient for the study of nonlocal transport properties, which require controlled approximations of the quantum solution on long time scales.

Author contribution statement

Both authors have contributed equally to all stages of this work.

Appendix A: Dyson equation in the bicoherent state representation

The aim of this Appendix is to prove equations (15)–(17). We first express the vortex Green's functions $g_{n_1,n_2}(\mathbf{R};t)$

in terms of the bicoherent Green's functions $g_{\boldsymbol{\rho}_1,\boldsymbol{\rho}_2}(\mathbf{R};t)$ by inverting the relation (14) thanks to the analytical dependence on the variables ζ_1 and ζ_2^*

$$g_{n_1,n_2}(\mathbf{R};t) = \int\frac{d^2\boldsymbol{\rho}_1}{2\pi l_B^2}\int\frac{d^2\boldsymbol{\rho}_2}{2\pi l_B^2}\left(\frac{\zeta_1^*}{\sqrt{2}l_B}\right)^{n_1}\left(\frac{\zeta_2}{\sqrt{2}l_B}\right)^{n_2} \times\frac{g_{\boldsymbol{\rho}_1,\boldsymbol{\rho}_2}(\mathbf{R};t)}{\sqrt{n_1!\,n_2!}}\,e^{-\frac{|\zeta_1|^2+|\zeta_2|^2}{4l_B^2}}. \quad (A.1)$$

This expression is then inserted into equation (5), which reads after summing over the integers n_1 and n_2

$$G(\mathbf{r},\mathbf{r}';t) = \int\frac{d^2\mathbf{R}}{2\pi l_B^2}\int\frac{d^2\boldsymbol{\rho}_1}{2\pi l_B^2}\int\frac{d^2\boldsymbol{\rho}_2}{2\pi l_B^2}\,g_{\boldsymbol{\rho}_1,\boldsymbol{\rho}_2}(\mathbf{R};t) \times e^{-(l_B^2/4)\Delta_{\mathbf{R}}}\left[\langle\boldsymbol{\rho}_2,\mathbf{R}|\mathbf{r}'\rangle\langle\mathbf{r}|\boldsymbol{\rho}_1,\mathbf{R}\rangle\right]. \quad (A.2)$$

We then reorganize the variables of integrations $\boldsymbol{\rho}_1$ and $\boldsymbol{\rho}_2$ in the set of variables $\boldsymbol{\rho}=(\rho_x,\rho_y)$ with $\rho_x = (\rho_{1x}+\rho_{2x})/2 - i(\rho_{2y}-\rho_{1y})/2$ and $\rho_y = (\rho_{1y}+\rho_{2y})/2 + i(\rho_{2x}-\rho_{1x})/2$, and $\boldsymbol{\rho}_- = \boldsymbol{\rho}_1 - \boldsymbol{\rho}_2$. Introducing the change in function

$$g_{\boldsymbol{\rho}_1,\boldsymbol{\rho}_2}(\mathbf{R};t) = \langle\boldsymbol{\rho}_1|\boldsymbol{\rho}_2\rangle\, e^{i(\boldsymbol{\rho}_-\times\hat{\mathbf{z}})\cdot\boldsymbol{\nabla}_{\boldsymbol{\rho}}}\, e^{(l_B^2/4)\Delta_{\boldsymbol{\rho}}} g(\boldsymbol{\rho},\mathbf{R};t), \quad (A.3)$$

and noting that

$$\langle\boldsymbol{\rho}_1|\boldsymbol{\rho}_2\rangle\langle\boldsymbol{\rho}_2,\mathbf{R}|\mathbf{r}'\rangle\langle\mathbf{r}|\boldsymbol{\rho}_1,\mathbf{R}\rangle = e^{-\frac{\boldsymbol{\rho}_-^2}{2l_B^2}}\langle\boldsymbol{\rho},\mathbf{R}|\mathbf{r}'\rangle\langle\mathbf{r}|\boldsymbol{\rho},\mathbf{R}\rangle, \quad (A.4)$$

we then perform the integration over the variable $\boldsymbol{\rho}_-$ in equation (A.2) to get the expression

$$G(\mathbf{r},\mathbf{r}';t) = \int\frac{d^2\mathbf{R}}{2\pi l_B^2}\int\frac{d^2\boldsymbol{\rho}}{2\pi l_B^2}\,e^{-(l_B^2/4)\Delta_{\boldsymbol{\rho}}}\left[g(\boldsymbol{\rho},\mathbf{R};t)\right] \times e^{-(l_B^2/4)\Delta_{\mathbf{R}}}\left[\langle\boldsymbol{\rho},\mathbf{R}|\mathbf{r}'\rangle\langle\mathbf{r}|\boldsymbol{\rho},\mathbf{R}\rangle\right]. \quad (A.5)$$

Integrating by parts, we finally arrive at the result written in equation (15).

The equation obeyed by the function $g(\boldsymbol{\rho},\mathbf{R};t)$ is obtained by projecting Dyson equation (7) onto the bicoherent state representation. After summing over the discrete Landau level indices we obtain

$$\left(i\hbar\partial_t \pm i0^+\right) g_{\boldsymbol{\rho}_1,\boldsymbol{\rho}_2}(\mathbf{R};t) - \int\frac{d^2\boldsymbol{\rho}_3}{2\pi l_B^2}\,w_{\boldsymbol{\rho}_1,\boldsymbol{\rho}_3}(\mathbf{R})\star_{\mathbf{R}} g_{\boldsymbol{\rho}_3,\boldsymbol{\rho}_2}(\mathbf{R};t) = \langle\boldsymbol{\rho}_1|\boldsymbol{\rho}_2\rangle\,\delta(t), \quad (A.6)$$

where

$$w_{\boldsymbol{\rho}_1,\boldsymbol{\rho}_2}(\mathbf{R}) = \hbar\omega_c\left(\frac{\zeta_1\zeta_2^*}{2l_B^2}+\frac{1}{2}\right)\langle\boldsymbol{\rho}_1|\boldsymbol{\rho}_2\rangle + \int d^2\mathbf{r}\,e^{-(l_B^2/4)\Delta_{\mathbf{R}}}\left[\langle\boldsymbol{\rho}_1,\mathbf{R}|\mathbf{r}\rangle\langle\mathbf{r}|\boldsymbol{\rho}_2,\mathbf{R}\rangle\right]V(\mathbf{r}).$$

The first term in the right-hand side of this latter expression corresponds to the rewriting of the Landau level kinetic energy contribution in the bicoherent state representation. Using the general dependence (14) of $g_{\boldsymbol{\rho}_3,\boldsymbol{\rho}_2}(\mathbf{R};t)$ on the variables $\boldsymbol{\rho}_2$ and $\boldsymbol{\rho}_3$ to perform the integrals over the variable $\boldsymbol{\rho}_3$ and setting $\boldsymbol{\rho}_1=\boldsymbol{\rho}_2\equiv\boldsymbol{\rho}$ in equation (A.6), we derive in a first stage a closed equation obeyed by the diagonal component Green's functions $g_{\boldsymbol{\rho},\boldsymbol{\rho}}(\mathbf{R};t)$

$$\left(i\hbar\partial_t \pm i0^+ - w_{\boldsymbol{\rho},\boldsymbol{\rho}}(\mathbf{R})\right)\star_{\mathbf{R}}\, e^{\frac{l_B^2}{2}(\overleftarrow{\partial}_{\rho_x}-i\overleftarrow{\partial}_{\rho_y})(\overrightarrow{\partial}_{\rho_x}+i\overrightarrow{\partial}_{\rho_y})} \times g_{\boldsymbol{\rho},\boldsymbol{\rho}}(\mathbf{R};t) = \delta(t). \quad (A.7)$$

Considering the change in function (A.3), we write down in a second stage from equation (A.7) a similar equation for the function

$$g(\boldsymbol{\rho},\mathbf{R};t) = e^{-(l_B^2/4)\Delta_{\boldsymbol{\rho}}} g_{\boldsymbol{\rho},\boldsymbol{\rho}}(\mathbf{R};t),$$

which only differs from the previous equation (A.7) in the structure of the infinite-order differential operator (this step is most easily done by going temporarily to the Fourier space following the calculations detailed in Appendix A of Ref. [34]). The final result is provided in equation (17), where

$$E(\boldsymbol{\rho},\mathbf{R}) = e^{-(l_B^2/4)\Delta_{\boldsymbol{\rho}}} w_{\boldsymbol{\rho},\boldsymbol{\rho}}(\mathbf{R}) = \frac{1}{2}m^*\omega_c^2\boldsymbol{\rho}^2 + \int d^2\mathbf{r}\,K(\mathbf{r},\mathbf{r};\boldsymbol{\rho},\mathbf{R})\,V(\mathbf{r}). \quad (A.8)$$

The contribution arising from the potential energy $V(\mathbf{r})$ can be further simplified, given that

$$\begin{aligned}&\int d^2\mathbf{r}\,K(\mathbf{r},\mathbf{r};\boldsymbol{\rho},\mathbf{R})\,V(\mathbf{r})\\ &= e^{-(l_B^2/4)(\Delta_{\mathbf{R}}+\Delta_{\boldsymbol{\rho}})}\int\frac{d^2\mathbf{r}}{2\pi l_B^2}\,e^{-\frac{(\mathbf{r}-[\boldsymbol{\rho}+\mathbf{R}])^2}{2l_B^2}}V(\mathbf{r})\\ &= e^{-(l_B^2/4)(\Delta_{\mathbf{R}}+\Delta_{\boldsymbol{\rho}})}e^{(l_B^2/2)\Delta_{\boldsymbol{\rho}+\mathbf{R}}}\,V(\boldsymbol{\rho}+\mathbf{R}) = V(\boldsymbol{\rho}+\mathbf{R}).\end{aligned}$$

This means that the quantity $E(\boldsymbol{\rho},\mathbf{R})$ is nothing but the classical expression for the total energy.

References

1. K. von Klitzing, Rev. Mod. Phys. **58**, 519 (1986)
2. K.S. Novoselov, A.K. Geim, S.V. Morozov, D. Jiang, M.I. Katsnelson, I.V. Grigorieva, S.V. Dubonos, A.A. Firsov, Nature (Lond.) **438**, 197 (2005)
3. Y. Zhang, Y.-W. Tan, H.L. Stormer, P. Kim, Nature (Lond.) **438**, 201 (2005)
4. J. Jobst, D. Waldmann, F. Speck, R. Hirner, D.K. Maude, T. Seyller, H.B. Weber, Phys. Rev. B **81**, 195434 (2010)
5. J. Falson, M. Kawasaki, Rep. Prog. Phys. **81**, 1 (2018)
6. H. Cao, J. Tian, I. Miotkowski, T. Shen, J. Hu, S. Qiao, Y.P. Chen, Phys. Rev. Lett. **108**, 216803 (2012)
7. M.M. Fogler, A.Yu. Dobin, V.I. Perel, B.I. Shklovskii, Phys. Rev. B **56**, 6823 (1997)
8. M. Flöser, B.A. Piot, C.L. Campbell, D.K. Maude, M. Henini, R. Airey, Z.R. Wasilewski, S. Florens, T. Champel, New J. Phys. **15**, 083027 (2013)
9. R.B. Laughlin, Phys. Rev. B **23**, 5632(R) (1981)
10. B.I. Halperin, Phys. Rev. B **25**, 2185 (1982)

11. P. Streda, J. Phys. C **15**, L717 (1982)
12. D.J. Thouless, M. Kohmoto, M. Nightingale, M. den Nijs, Phys. Rev. Lett. **49**, 405 (1982)
13. D.J. Thouless, Phys. Rev. B **27**, 6083 (1984)
14. A.H. MacDonald, P. Streda, Phys. Rev. B **29**, 1616 (1984)
15. R.E. Prange, S.M. Girvin (Eds.), *The Quantum Hall Effect* (Springer, New York, 1987)
16. M. Büttiker, Phys. Rev. B **38**, 9375 (1988)
17. M. Janssen, O. Viehweger, U. Fastenrath, J. Hadju, *Introduction to the Theory of the Integer Quantum Hall Effect* (VCH, Germany, 1994)
18. B. Huckestein, Rev. Mod. Phys. **67**, 357 (1995)
19. I.A. Dmitriev, F. Evers, I.V. Gornyi, A.D. Mirlin, D.G. Polyakov, P. Wölfle, Phys. Status Solidi B **245**, 239 (2008)
20. V. Fock, Z. Phys. **47**, 446 (1928)
21. C.G. Darwin, Proc. Camb. Philos. Soc. **27**, 86 (1931)
22. L. Landau, Z. Phys. **64**, 629 (1930)
23. H.A. Fertig, B.I. Halperin, Phys. Rev. B **36**, 7969 (1987)
24. M. Büttiker, Phys. Rev. B **41**, 7906(R) (1990)
25. J.K. Jain, S. Kivelson, Phys. Rev. B **37**, 4111 (1988)
26. A. Entelis, S. Levit, Phys. Rev. Lett. **69**, 3001 (1992)
27. V. Kagalovsky, Phys. Rev. B **53**, 13656 (1996)
28. T. Tochishita, M. Mizui, M.H. Kuratsuji, Phys. Lett. A **212**, 304 (1996)
29. P. Krasón, J. Milewski, Acta Phys. Pol. A **132**, 94 (2017)
30. I.A. Malkin, V.I. Man'ko, Sov. Phys. JETP **28**, 527 (1969)
31. T. Champel, S. Florens, Phys. Rev. B **75**, 245326 (2007)
32. T. Champel, S. Florens, L. Canet, Phys. Rev. B **78**, 125302 (2008)
33. T. Champel, S. Florens, Phys. Rev. B **80**, 161311(R) (2009)
34. T. Champel, S. Florens, Phys. Rev. B **80**, 125322 (2009)
35. T. Champel, S. Florens, Phys. Rev. B **82**, 045021 (2010)
36. K. Hashimoto, C. Sohrmann, J. Wiebe, T. Inaoka, F. Meier, Y. Hirayama, R.A. Römer, R. Wiesendanger, M. Morgenstern, Phys. Rev. Lett. **101**, 256802 (2008)
37. K. Hashimoto, T. Champel, S. Florens, C. Sohrmann, J. Wiebe, Y. Hirayama, R.A. Römer, R. Wiesendanger, M. Morgenstern, Phys. Rev. Lett. **109**, 116805 (2012)
38. F. Bayen, M. Flato, C. Fronsdal, A. Lichnerowicz, D. Sternheimer, Ann. Phys. (N.Y.) **111**, 61 (1978)
39. F. Bayen, M. Flato, C. Fronsdal, A. Lichnerowicz, D. Sternheimer, Ann. Phys. (N.Y.) **111**, 111 (1978)
40. C.K. Zachos, D.B. Fairlie, T.L. Curtright (Eds.), *Quantum Mechanics in Phase Space: An Overview with Selected Papers*, World Scientific Series in 20th Century Physics (World Scientific, Singapore, 2005), Vol. 34
41. A. Feldman, A.H. Kahn, Phys. Rev. B **1**, 4584 (1970)
42. S. Varro, J. Phys. A: Math. Gen. **17**, 1631 (1984)
43. V.I. Man'ko, E.D. Zhebrak, Opt. Spectrosc. **113**, 624 (2012)
44. E.D. Zhebrak, Phys. Scr. **T153**, 014063 (2013)
45. T. Champel, S. Florens, M.E. Raikh, Phys. Rev. B **83**, 125321 (2011)